Computational mechanics and stochastic simulation of random polycrystals

N. Venkovic
nvenkov1@jhu.edu

Graduate Board Oral Exam
December 11, 2017

Motivation

Different morphologies lead to different mechanical behaviors.

Morphological statistics of single grains

Periodic viscoplastic polycrystal subjected to $\overline{\varepsilon}(t) \propto t\underline{e}_1 \otimes \underline{e}_1$

In-grain equivalent plastic strain densities

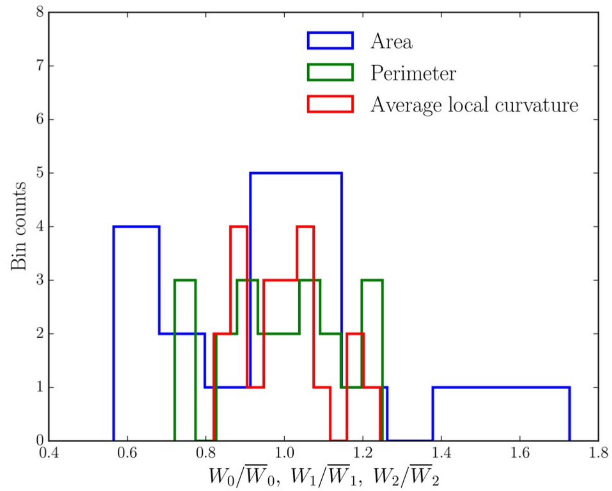

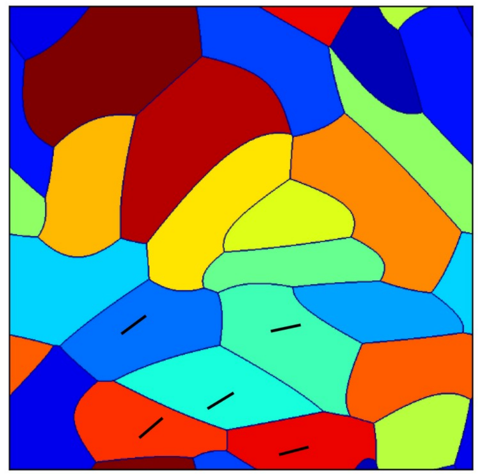

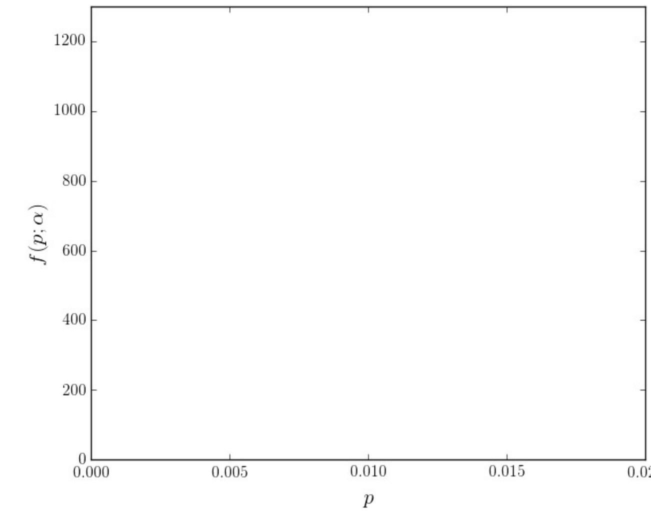

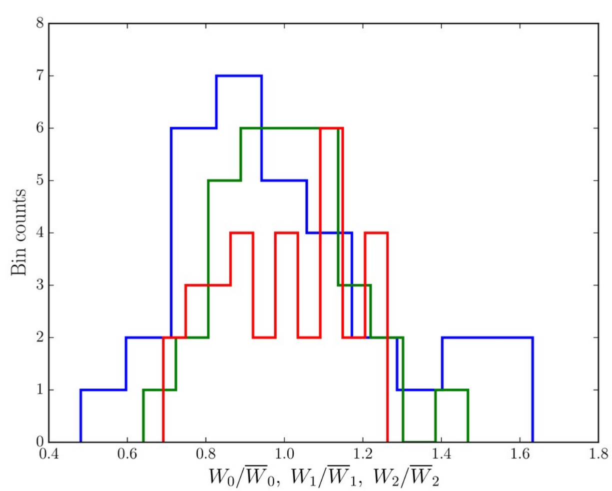

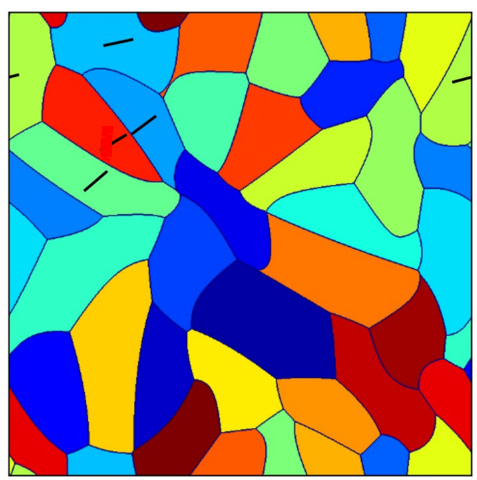

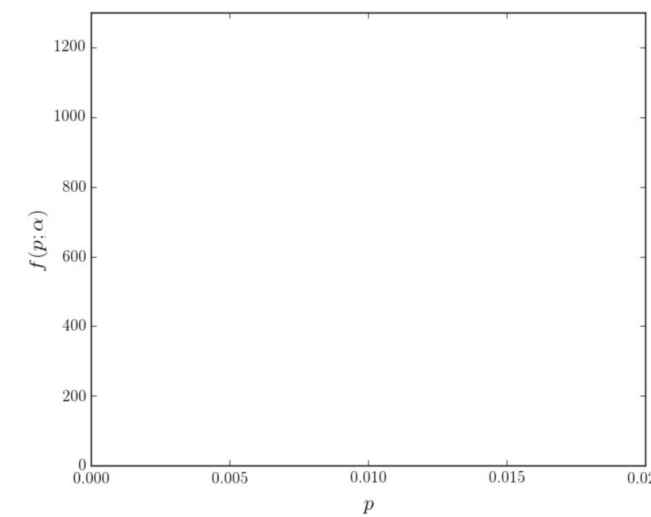

Motivation

Different morphologies lead to different mechanical behaviors.

Morphological statistics of single grains

Periodic viscoplastic polycrystal subjected to $\overline{\varepsilon}(t) \propto t\underline{e}_1 \otimes \underline{e}_1$

In-grain equivalent plastic strain densities

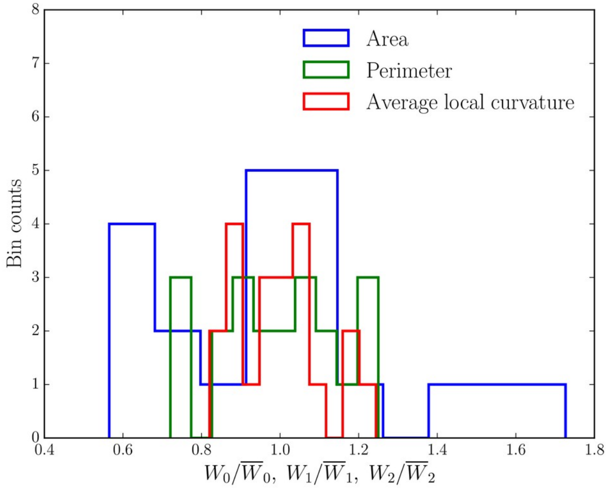

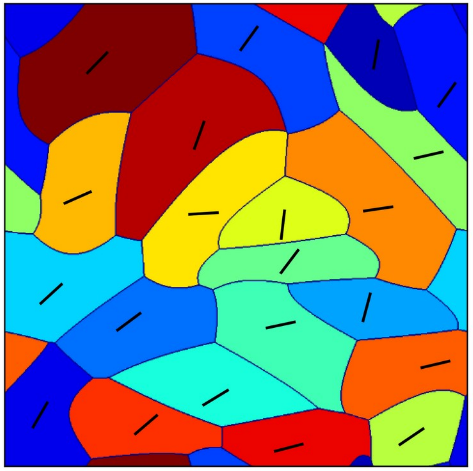

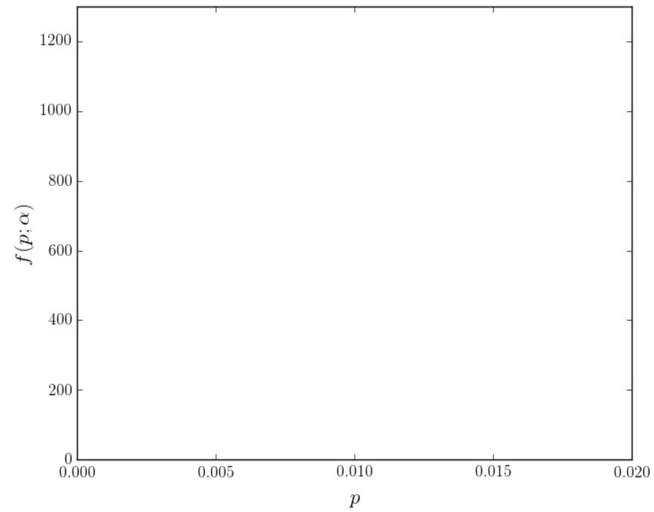

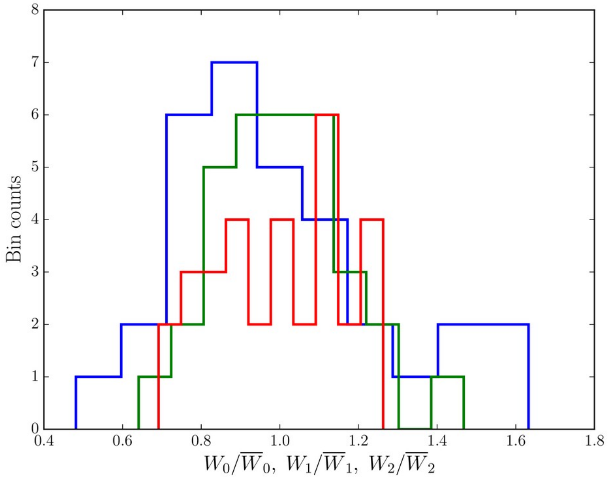

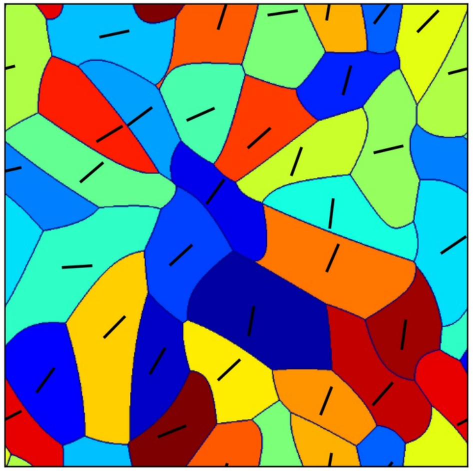

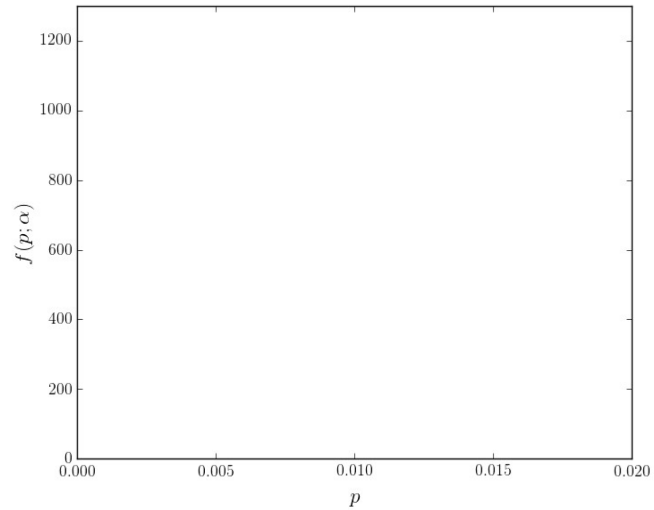

Motivation

Different morphologies lead to different mechanical behaviors.

Morphological statistics of single grains

Periodic viscoplastic polycrystal subjected to $\overline{\varepsilon}(t) \propto t \underline{e}_1 \otimes \underline{e}_1$

In-grain equivalent plastic strain densities

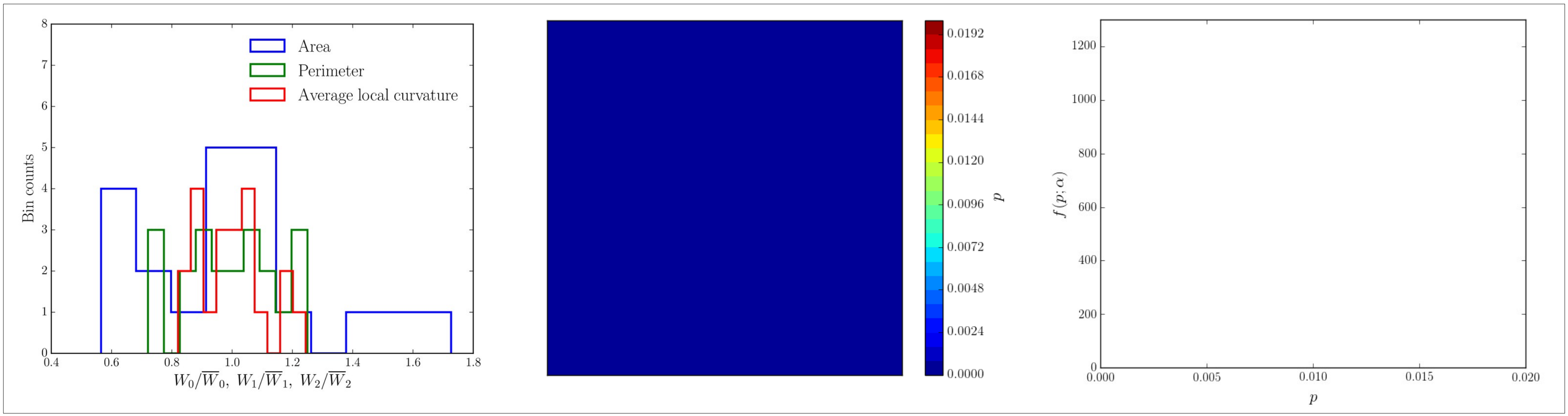

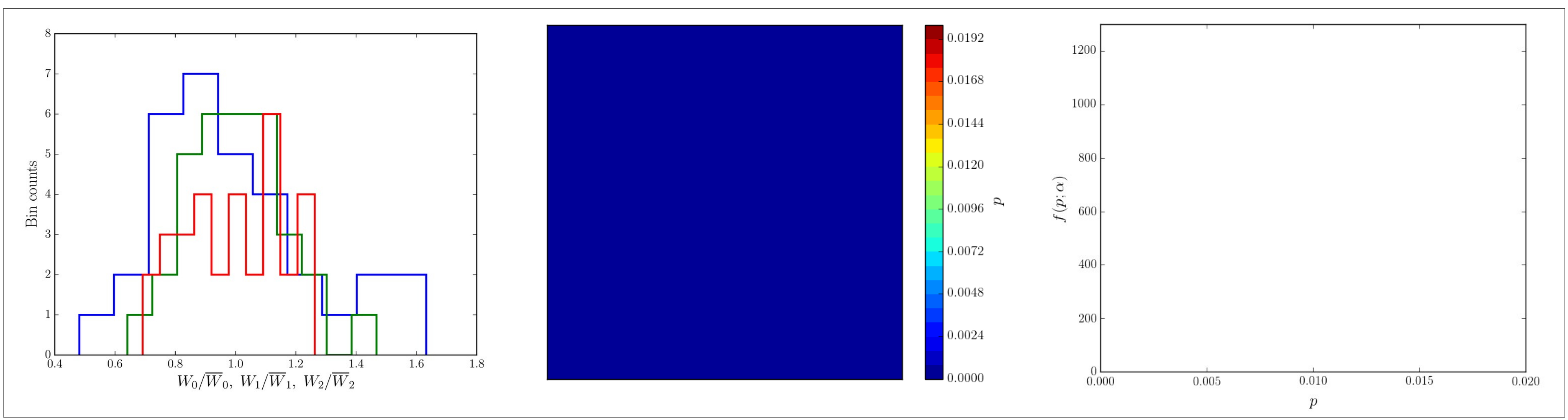

Motivation

Different morphologies lead to different mechanical behaviors.

Morphological statistics of single grains

Periodic viscoplastic polycrystal subjected to $\overline{\varepsilon}(t) \propto t\underline{e}_1 \otimes \underline{e}_1$

In-grain equivalent plastic strain densities

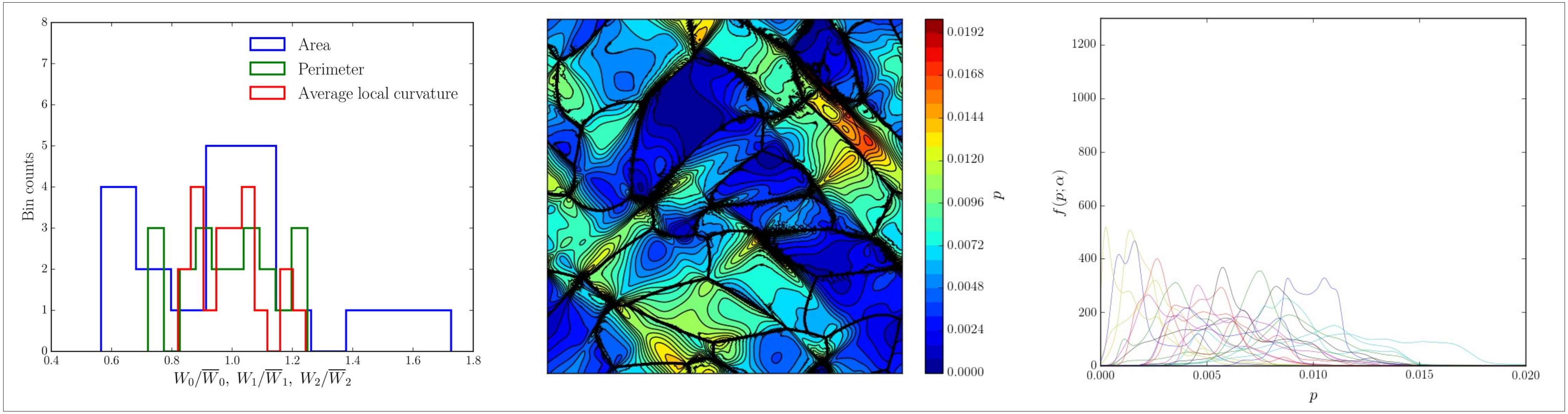

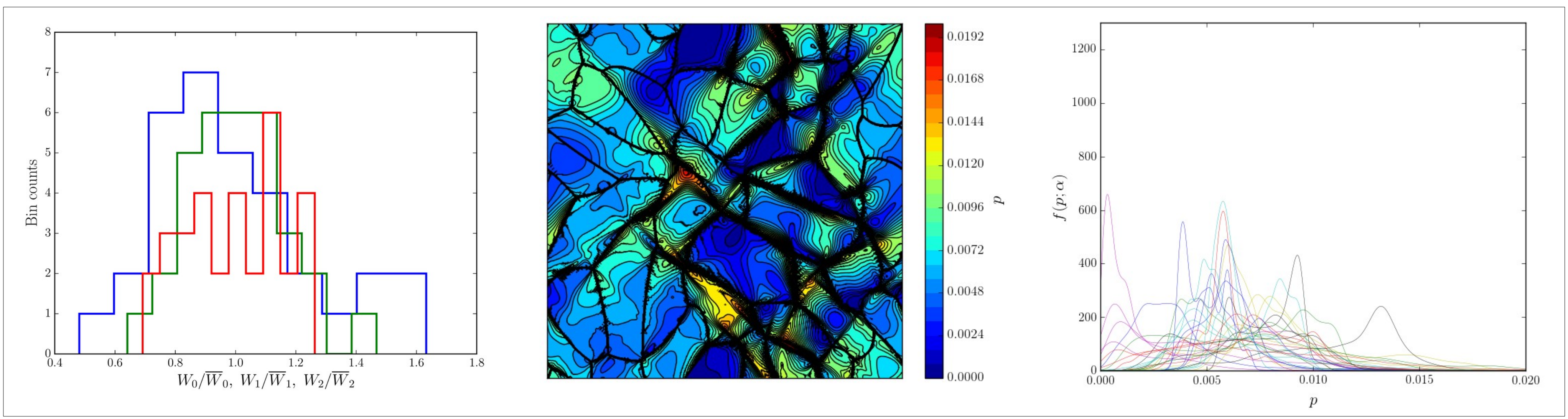

Motivation

Different morphologies lead to different mechanical behaviors.

Morphological statistics of single grains

Periodic viscoplastic polycrystal subjected to $\overline{\varepsilon}(t) \propto t\underline{e}_1 \otimes \underline{e}_1$

In-grain equivalent plastic strain densities

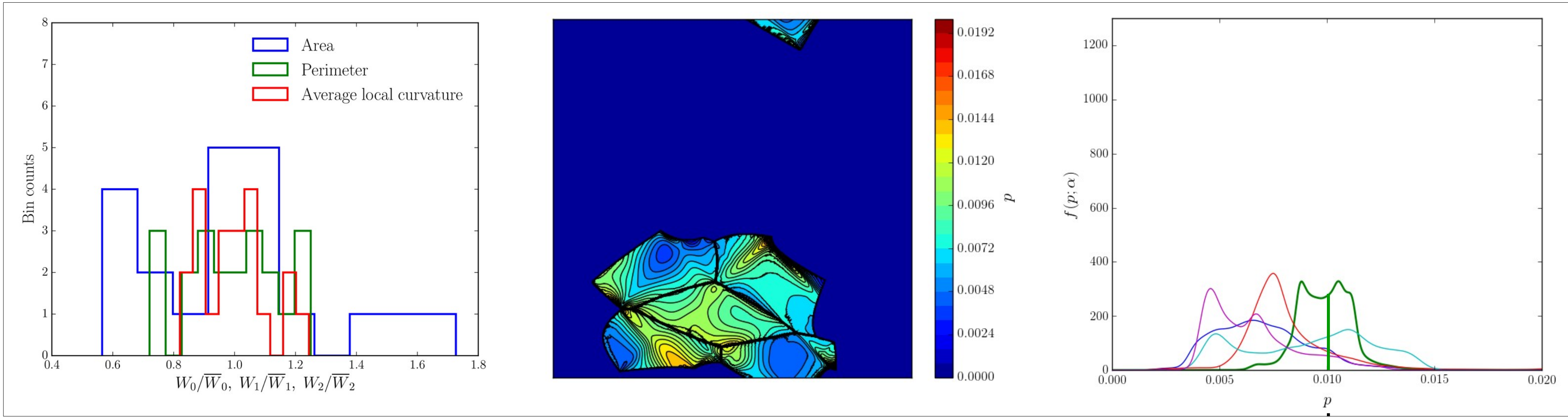

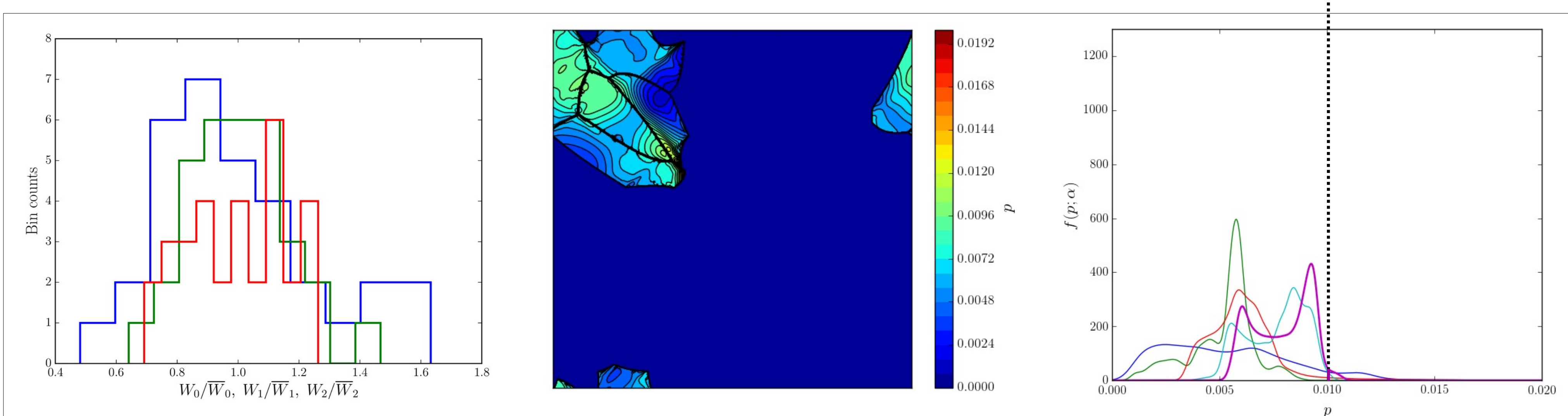

Outline of methodology

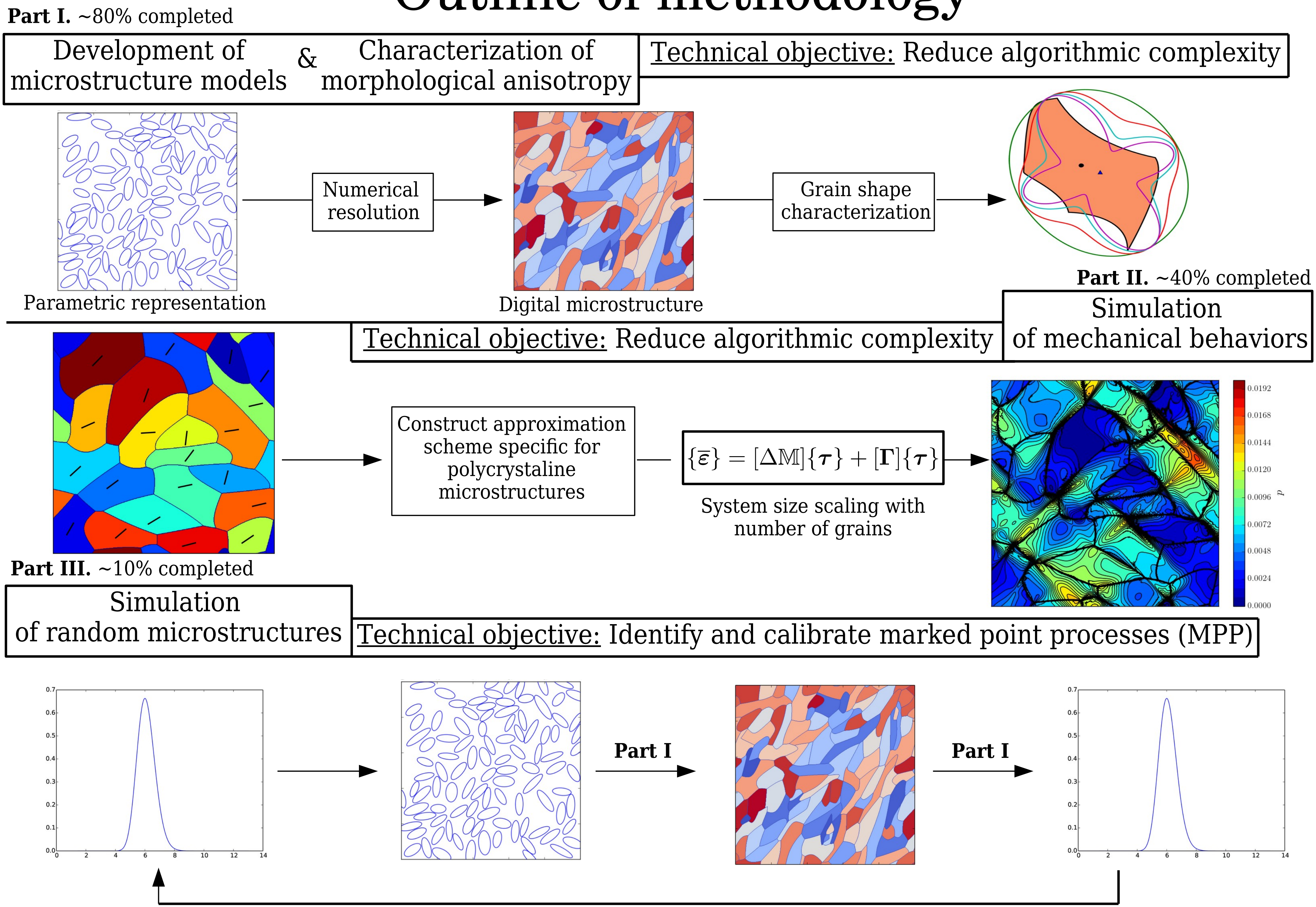

Part I. Parametric representation

Consider a pattern of n_α marked points

$$\Xi = \{(\underline{x}_\alpha, \mathbf{Z}_\alpha) \mid 1 \leq \alpha \leq n_\alpha,\ \mathbf{Z}_\alpha \succ 0\}$$

The underlying microstructure $\mathrm{Tess}(\Xi)$ is a partition of space into n_α cells (or grains)

$$\Omega_\alpha = \{\underline{x} \,|\operatorname*{argmin}_\gamma\, (\underline{x} - \underline{x}_\gamma) \cdot \mathbf{Z}_\gamma \cdot (\underline{x} - \underline{x}_\gamma) = \alpha\}$$

Marked point pattern (MPP)

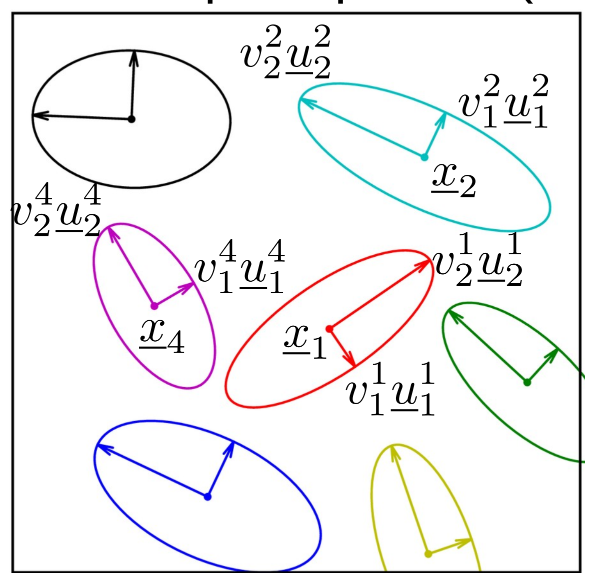

$$\mathbf{Z}_\alpha = \frac{\underline{u}_1^\alpha \otimes \underline{u}_1^\alpha}{(v_1^\alpha)^2} + \frac{\underline{u}_2^\alpha \otimes \underline{u}_2^\alpha}{(v_2^\alpha)^2}$$

Numerical Resolution

Underlying microstructure

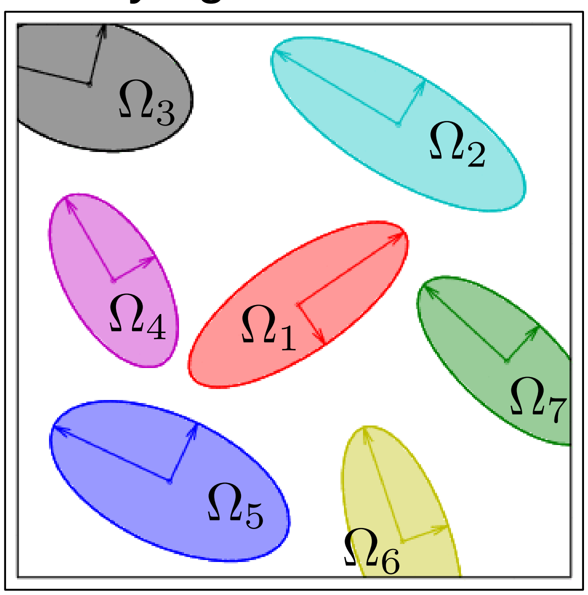

Part I. Parametric representation

Consider a pattern of n_α marked points

$$\Xi = \{(\underline{x}_\alpha, \mathbf{Z}_\alpha) \mid 1 \leq \alpha \leq n_\alpha,\ \mathbf{Z}_\alpha \succ 0\}$$

The underlying microstructure $\mathrm{Tess}(\Xi)$ is a partition of space into n_α cells (or grains)

$$\Omega_\alpha = \{\underline{x} \,|\operatorname*{argmin}_\gamma\ (\underline{x} - \underline{x}_\gamma) \cdot \mathbf{Z}_\gamma \cdot (\underline{x} - \underline{x}_\gamma) = \alpha\}$$

Marked point pattern (MPP)

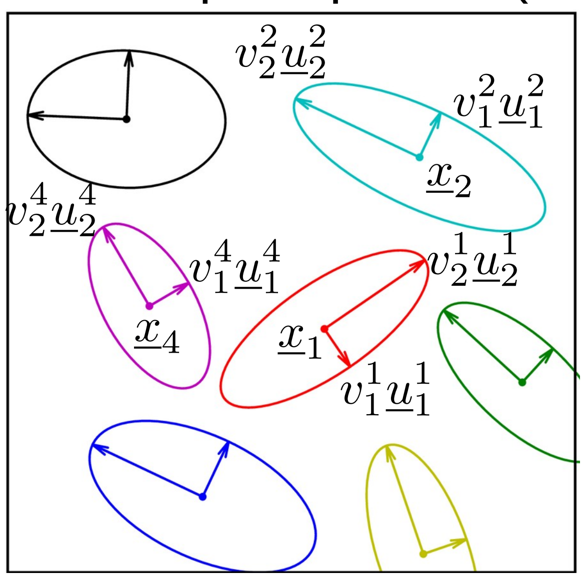

$$\mathbf{Z}_\alpha = \frac{\underline{u}_1^\alpha \otimes \underline{u}_1^\alpha}{(v_1^\alpha)^2} + \frac{\underline{u}_2^\alpha \otimes \underline{u}_2^\alpha}{(v_2^\alpha)^2}$$

Numerical Resolution

Underlying microstructure

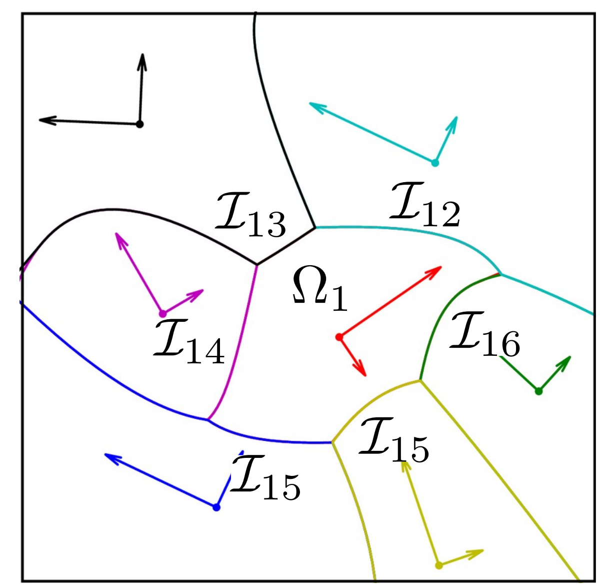

Every cell Ω_α has a boundary $\partial\Omega_\alpha$ partitioned into common curves $\mathcal{I}_{\alpha\gamma}$ shared with neighbors its Ω_γ .

Part I. Morphological characterization

Single grains are characterized using Minkowski tensors:

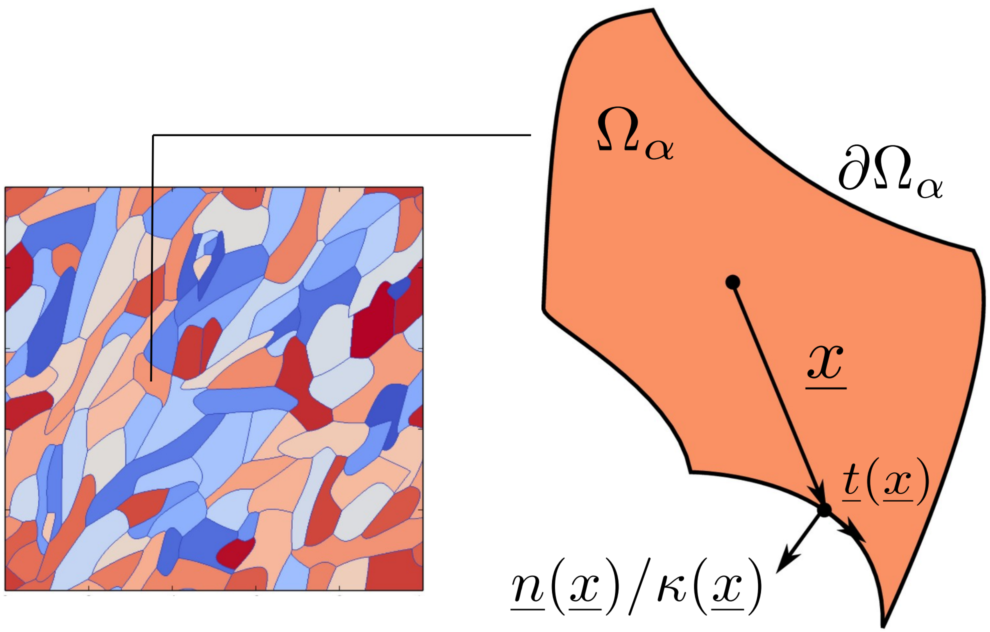

Measures of mass distribution:

$$\mathcal{W}_0^{r,0} = \int_{\Omega_\alpha} \underline{x}^{\otimes^r} \mathrm{d}V$$

Measures of surface distribution:

$$\mathcal{W}_1^{r,s} = \int_{\partial\Omega_\alpha} \underline{x}^{\otimes^r} \odot [\underline{n}(\underline{x})]^{\otimes^s} \mathrm{d}S$$

Curvature-weighted measures of surface distribution:

$$\mathcal{W}_2^{r,s} = \int_{\partial\Omega_\alpha} \kappa(\underline{x}) \underline{x}^{\otimes^r} \odot [\underline{n}(\underline{x})]^{\otimes^s} \mathrm{d}S$$

Examples of projection up to order 8

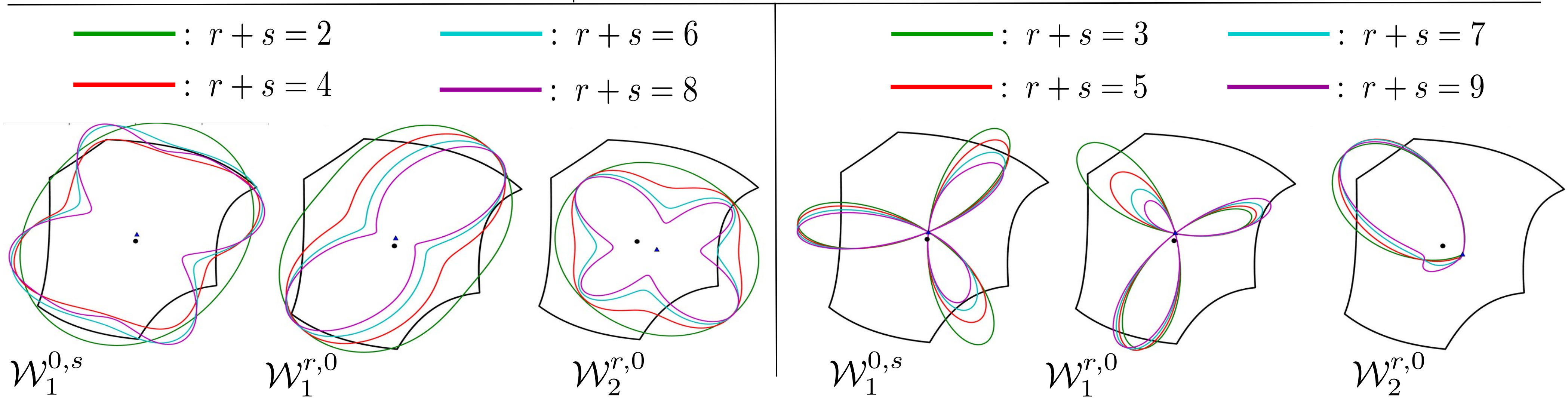

Part I. Numerical resolution – naive approach

1) Discretize the domain into n pixels

2) Proceed as follows pixel-by-pixel

Compute contact times, attribute pixel,

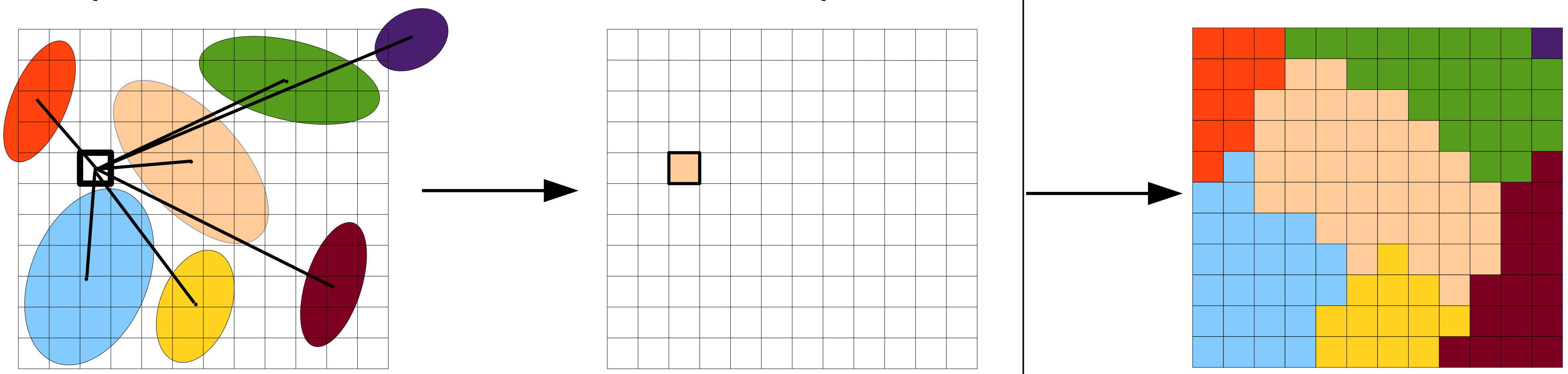

Resulting algorithm has complexity $O(n)$. How large need n be?

<u>Poor boundary resolution</u>

Small n

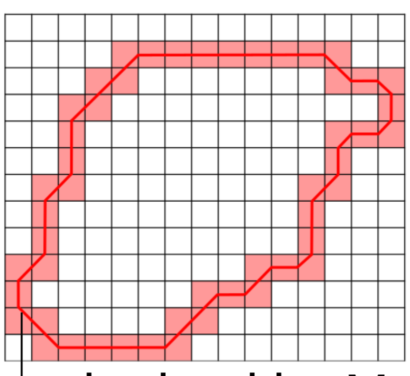

Actual boundary

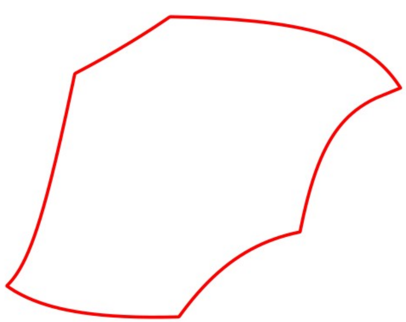

obtained by Marching squares

<u>Mislabeling</u>

Small n

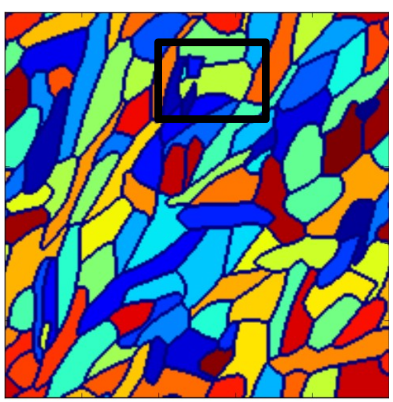

Large n

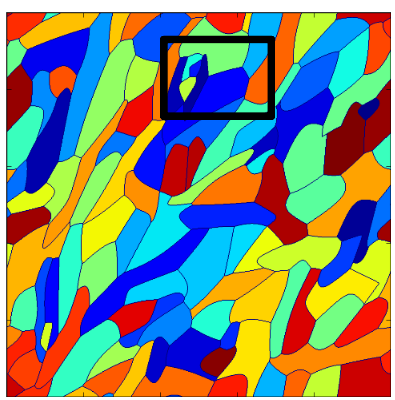

Part I. Transformation of the problem

Instead of discretizing the plane and solving for approximations of Ω_α, we transform the problem as follows

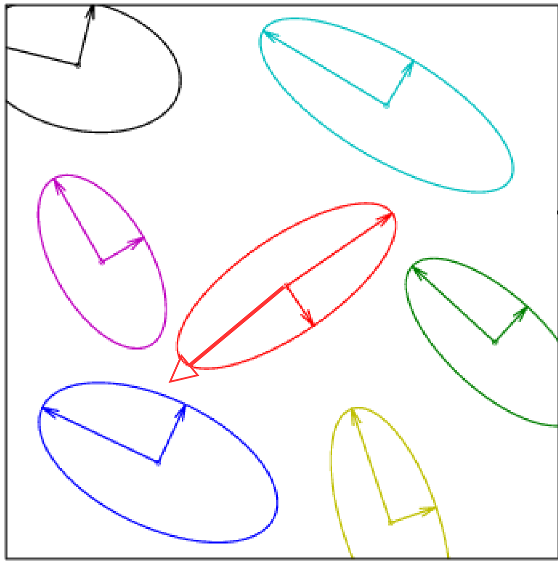

$$\phi^\alpha_\gamma : (\theta_a, \theta_b) \to S^1 \times (0, \Delta)$$
$$: \theta \mapsto (\underline{x}(\theta), \xi^\alpha_\gamma \circ \underline{x}(\theta))$$

ξ^α_γ is given in terms of $\mathbf{Z}_\alpha$ and $\mathbf{Z}_\gamma$
.

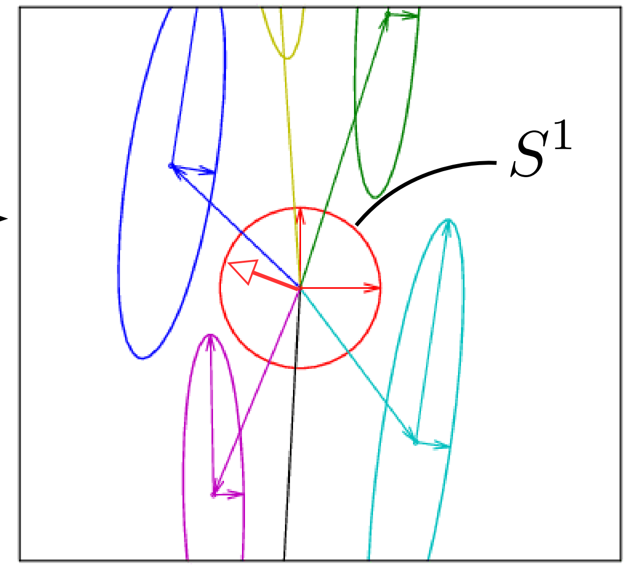

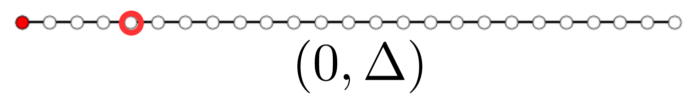

and try to solve for the curves $\mathcal{I}_{\alpha\gamma} \subset \partial\Omega_\alpha$.

Solving for the transformed problem is equivalent to solve for the overlay of the functions ξ^α_γ of the neighbors Ω_γ of Ω_α.

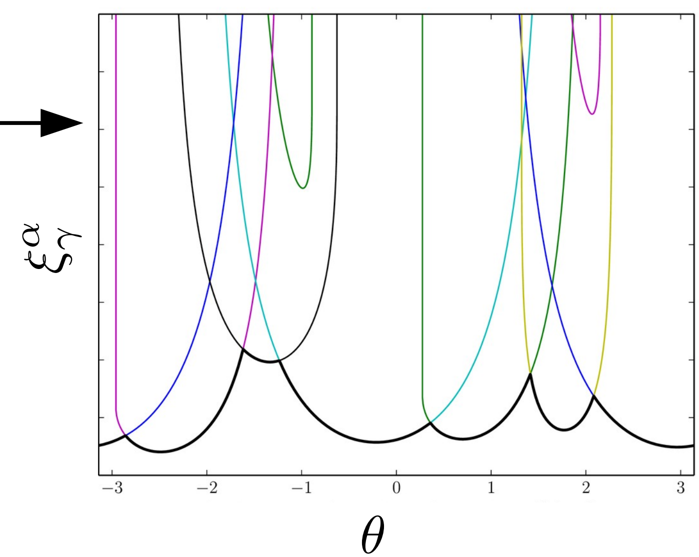

But, what are the neighbors of Ω_α?

Part I. Enriched Marching Squares (EMS)

Digital microstructure — Marching square (MS) algorithms → Approximate grain boundaries

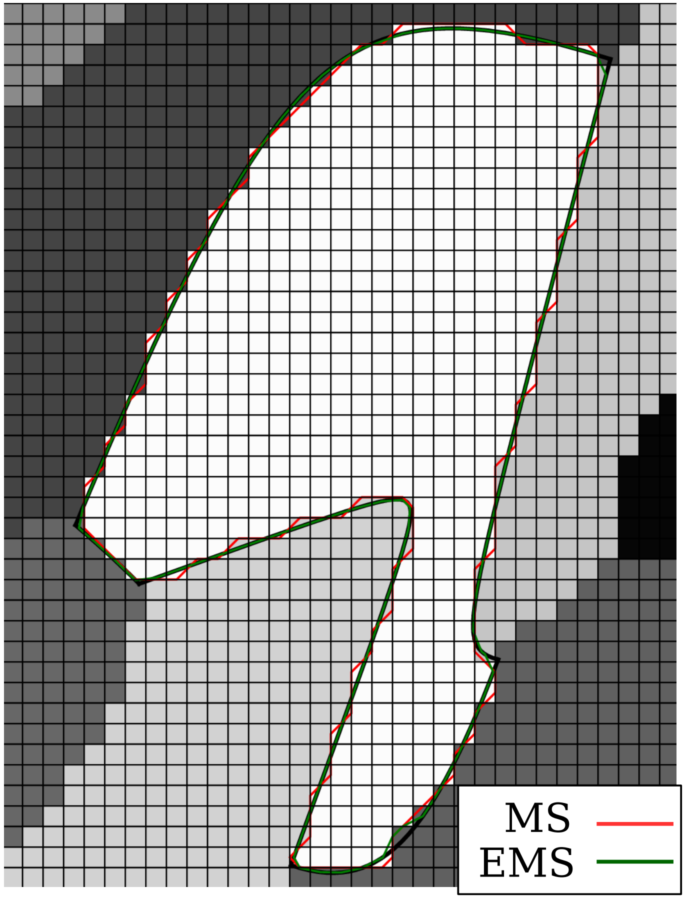

Using our analytical solution for the grain boundary, we obtain an enriched MS (EMS)

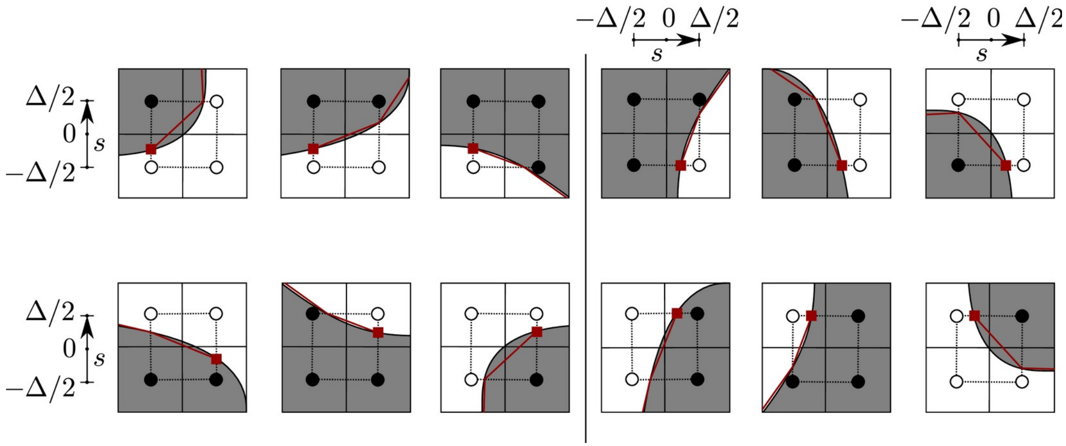

Expressions of Minkowski tensors:

$$\mathcal{W}_0^{r,0} = \frac{1}{r+2}\sum_{k=1}^{n}\sum_{i=0}^{r+1}\sum_{j=0}^{i}\binom{r+1}{i}\binom{i}{j}\frac{(-1)^{i-j}L_k}{i+1}\left[\underline{v}_k^{\otimes^{r+1-j}} \odot \underline{v}_{k+1}^{\otimes^{j}}\right]\cdot \underline{n}_k,$$

$$L_k = \|\underline{v}_{k+1} - \underline{v}_k\|$$

$$\mathcal{W}_1^{r,s} = \frac{1}{2}\sum_{k=1}^{n}\sum_{i=0}^{r}\sum_{j=0}^{i}\binom{r}{i}\binom{i}{j}\frac{(-1)^{i-j}L_k}{i+1}\underline{v}_k^{\otimes^{r-j}} \odot \underline{v}_{k+1}^{\otimes^{j}} \odot \underline{n}_k^{\otimes^{s}},$$

$$\mathcal{W}_2^{r,s} = \frac{1}{2}\sum_{k=1}^{n}\sum_{i=0}^{s}\sum_{j=0}^{i}\binom{s}{i}\binom{i}{j}\frac{(-1)^{i-j}}{L_k^{i}}\underline{v}_k^{\otimes^{i-j}} \odot \underline{v}_{k+1}^{\otimes^{r+j}} \odot \underline{n}_k^{\otimes^{s-i}} I_k^{s,i}(\Delta\theta_k)$$

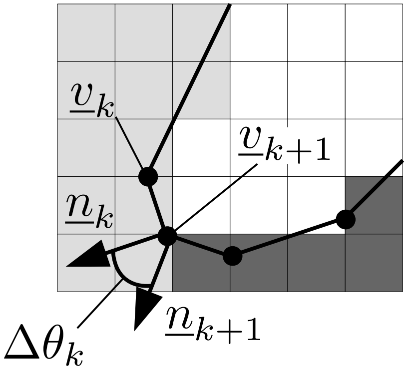

Part I. Expressions of Minkowski tensors

If the expressions of the common curves and the common points are known, there is no need to approximate the boundaries using an MS algorithm. We have

$\underline{x}_\alpha$, $\underline{u}_1^\alpha$ and $\underline{u}_2^\alpha$ are from the MPP.

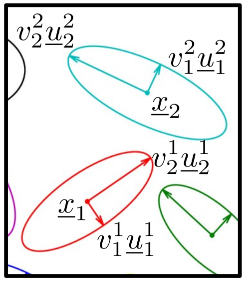

$$\mathcal{W}_0^{r,0} = \sum_{i=0}^{r}\sum_{j=0}^{r-i}\binom{r}{i+j}\underline{x}_\alpha^{\otimes^{r-i-j}} \odot \underline{u}_1^{\alpha^{\otimes^{i}}} \odot \underline{u}_2^{\alpha^{\otimes^{j}}}\, I_0^{i,j}$$

$$\mathcal{W}_1^{r,s} = \sum_{i=0}^{r}\sum_{j=0}^{r-i}\sum_{k=0}^{s}\binom{r}{i+j}\binom{s}{k}\underline{x}_\alpha^{\otimes^{r-i-j}} \odot \underline{u}_1^{\alpha^{\otimes^{s+i-k}}} \odot \underline{u}_2^{\alpha^{\otimes^{j+k}}}\, I_1^{i,j,k,s-k}$$

$$\mathcal{W}_2^{r,s} = \sum_{i=0}^{r}\sum_{j=0}^{r-i}\sum_{k=0}^{s}\binom{r}{i+j}\binom{s}{k}\underline{x}_\alpha^{\otimes^{r-i-j}} \odot \underline{u}_1^{\alpha^{\otimes^{s+i-k}}} \odot \underline{u}_2^{\alpha^{\otimes^{j+k}}}\, I_2^{i,j,k,s-k} + \underbrace{\sum_{\underline{y}\in\mathcal{K}_\alpha}\mathcal{D}^{r,s}(\underline{y})}_{\text{Effect of common points}}$$

where $I_0^{i,j}$ and $I_\nu^{i,j,k,l}$ are scalar coefficients obtained by integrating the functions ξ_γ^α defined for the neighbors Ω_γ of Ω_α.

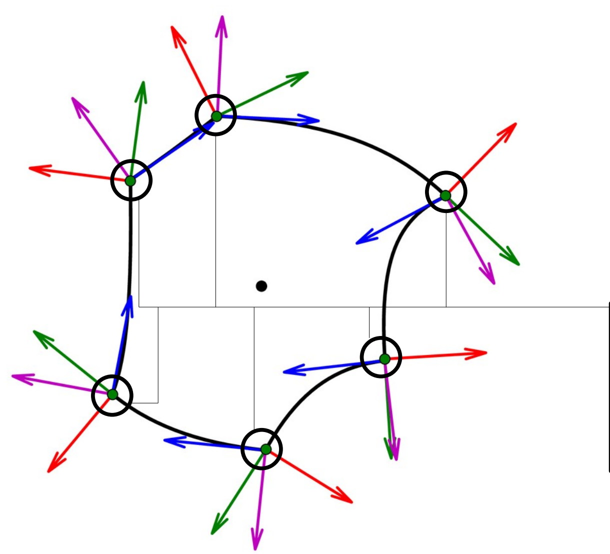

Part II. Periodic Lippmann-Schwinger problems

Periodic elastic Cauchy-Navier problem:

$$\boxed{\begin{array}{l} \boldsymbol{\sigma}(\underline{x}) = \mathbb{L}(\underline{x}) : \boldsymbol{\varepsilon}(\underline{x}) \ , \qquad \nabla \cdot \boldsymbol{\sigma}(\underline{x}) = \underline{0} \ , \qquad \boldsymbol{\varepsilon}(\underline{x}) = \{\nabla \underline{u}(\underline{x})\}_{sym} \\ \quad \text{with } \mathbb{L}(\underline{x} + (n\underline{e}_1 + m\underline{e}_2)L) = \mathbb{L}(\underline{x}) \text{ for all } \underline{x} \in \mathbb{R}^2 \text{ and } n, m \in \mathbb{Z} \ , \\ \quad \text{and } \boldsymbol{\sigma}(\underline{x} + (n\underline{e}_1 + m\underline{e}_2)) \cdot \underline{e}_k = \boldsymbol{\sigma}(\underline{x}) \cdot \underline{e}_k \ , \\ \quad \text{subjected to } \overline{\boldsymbol{\varepsilon}} = \boldsymbol{\varepsilon}_0. \qquad \boxed{\text{Original pb.}} \end{array}}$$

where $\overline{\bullet} := \dfrac{1}{L^2}\displaystyle\int_\Omega \bullet(\underline{x}) \mathrm{d}\nu_{\underline{x}}$ and $\Omega := [0, L] \times [0, L]$.

Introduce a polarization field $\boldsymbol{\tau}$ with reference $\mathbb{L}^0$,

$$\boldsymbol{\tau}(\underline{x}) := \boldsymbol{\sigma}(\underline{x}) - \mathbb{L}^0 : \boldsymbol{\varepsilon}(\underline{x}) = [\mathbb{L}(\underline{x}) - \mathbb{L}^0] : \boldsymbol{\varepsilon}(\underline{x}) = \Delta\mathbb{L}(\underline{x}) : \boldsymbol{\varepsilon}(\underline{x})$$

leads to a Periodic elastic Lippmann-Schwinger problem:

$$\boxed{\nabla \cdot \boldsymbol{\tau}(\underline{x}) + \nabla \cdot [\mathbb{L}^0 : \boldsymbol{\varepsilon}(\underline{x})] = \underline{0} \qquad \boxed{\text{Auxiliary pb.}}}$$

with solution

$$\boxed{\boldsymbol{\varepsilon}(\underline{x}) = \overline{\boldsymbol{\varepsilon}} - \boldsymbol{\Gamma} * \boldsymbol{\tau}(\underline{x}) = \overline{\boldsymbol{\varepsilon}} - \boldsymbol{\Gamma} * [\Delta\mathbb{L} : \boldsymbol{\varepsilon}(\underline{x})]}$$

Periodic Green operator for strains.

where $\boldsymbol{\Gamma} * \boldsymbol{\tau}(\underline{x}) := \displaystyle\int_{\mathbb{R}^2} \boldsymbol{\Gamma}(\underline{x}' - \underline{x}) : \boldsymbol{\tau}(\underline{x}') \ \mathrm{d}\nu_{\underline{x}'}$ is a convolution of $\boldsymbol{\Gamma}(\Delta\underline{x})$.

Part II. Basic approximation scheme

FFT-based iterative scheme:

$$\boldsymbol{\tau}(\underline{x}) \leftarrow \Delta\mathbb{L}(\underline{x}) : \boldsymbol{\varepsilon}_0$$

$$^{0}\boldsymbol{\tau}(\underline{x}) \leftarrow \boldsymbol{\tau}(\underline{x})$$

$$\text{while } \ \|\overline{\nabla \cdot \boldsymbol{\sigma}}\| > tol :$$

$$\quad \hat{\hat{\varepsilon}}(\underline{0}) \leftarrow \mathbf{0}$$

$$\quad \hat{\hat{\varepsilon}}(\underline{\omega}) \leftarrow -\hat{\boldsymbol{\Gamma}}(\underline{\omega}) : \mathcal{FFT}\{\boldsymbol{\tau}(\underline{x})\}(\underline{\omega}) \ \forall \ \underline{\omega} \neq \underline{0}$$

$$\quad \boldsymbol{\tau}(\underline{x}) \leftarrow {}^{0}\boldsymbol{\tau}(\underline{x}) + \Delta\mathbb{L}(\underline{x}) : \mathcal{FFT}^{-1}\{\hat{\hat{\varepsilon}}(\underline{\omega})\}(\underline{x})$$

Pros:
- Easy pre-processing,
- Compatible with anelastic eigenstrain formulations.

Cons:
- Uses a lot of memory,
- Post-processing is data intensive,
- No explicit insight about morphology,
- Complexity is $O(n \log n)$ per iteration, for n pixels.

Instead, we want a scheme that

- is especially tailored to polycrystalline microstructures,
- has complexity governed by the number of grains
- carries information about the morphology
- is easy to post-process.

How large need n be?
How many iterations are enough?

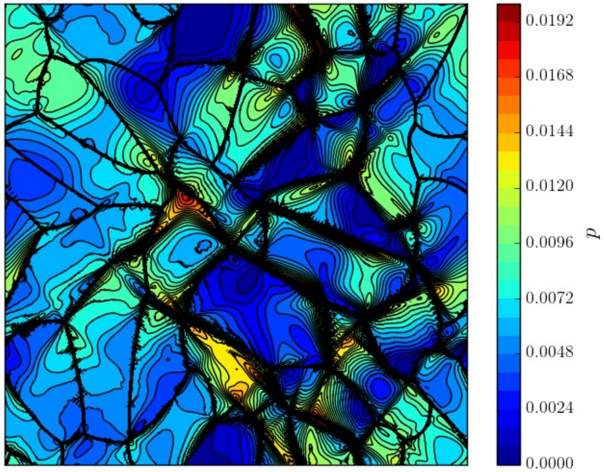

Part II. Hashin-Shtrikman variational principle

Consider the Hashin-Shtrikman (HS) functional given by

$$2\mathcal{H}(\boldsymbol{\tau}) := \boldsymbol{\varepsilon}_0 : \mathbb{L}_0 : \boldsymbol{\varepsilon}_0 + \overline{(2\boldsymbol{\tau} : \boldsymbol{\varepsilon}_0 - \boldsymbol{\tau} : (\Delta\mathbb{L})^{-1} : \boldsymbol{\tau} - \boldsymbol{\tau} : (\boldsymbol{\Gamma} * \boldsymbol{\tau}))}$$

(1) Assuming an equilibrated polarization, i.e. $\boldsymbol{\varepsilon}(\underline{x}) = \overline{\boldsymbol{\varepsilon}} - \boldsymbol{\Gamma} * \boldsymbol{\tau}(\underline{x})$, $\mathcal{H}(\boldsymbol{\tau})$ is stationary at $\boldsymbol{\tau}(\underline{x}) = \Delta\mathbb{L} : \boldsymbol{\varepsilon}(\underline{x})$, irrespectively of $\mathbb{L}_0$:

The solution to the Lippmann-Schwinger problem is a stationary point of the HS functional.

(2) Hashin and Shtrikman (1962) proved that

$$\Delta\mathbb{L}(\underline{x}) \prec 0 \quad \Longrightarrow \quad \mathcal{H}(\boldsymbol{\tau}) \text{ is strictly convex}$$

Okay. Then, let's consider a piecewise polynomial ansatz

Symmetric tensor of order k+2

$$\boldsymbol{\tau}^{h_p}(\underline{x}) := \sum_{\alpha} \chi_\alpha(\underline{x}) \sum_{k=0}^{p} \left\langle \boldsymbol{\tau}^\alpha \boldsymbol{\partial}^k, (\underline{x} - \underline{x}^\alpha)^{\otimes k} \right\rangle_k$$

for some *p* and solve for the minimizer $\{\boldsymbol{\tau}^\alpha \boldsymbol{\partial}^k, 0 \le k \le p\}$ of $\mathcal{H}(\boldsymbol{\tau}^{h_p})$.

Part II. Implementation & validation

Note that $\mathcal{H}(\boldsymbol{\tau}^{h_p})$ is a quadratic form. Consequently, the minimizer $\{\boldsymbol{\tau}^{\alpha}\boldsymbol{\partial}^{k}, 0 \leq k \leq p\}$ is solution of the linear system

$$\underset{N\times 1}{\{\overline{\boldsymbol{\varepsilon}}\}} = \underset{N\times N}{[\Delta\mathbb{M}]}\underset{N\times 1}{\{\boldsymbol{\tau}\}} + \underset{N\times N}{[\boldsymbol{\Gamma}]}\underset{N\times 1}{\{\boldsymbol{\tau}\}}$$

where $N = 3n_{\alpha}\binom{p+2}{2}$.

in which $[\Delta\mathbb{M}]_{ij} \propto$ components of $\Delta\mathbb{M}^{\alpha} \otimes \mathcal{W}_0^{r,0}(\Omega_{\alpha})$ with $r \leq 2p$

with $r \leq 2p$

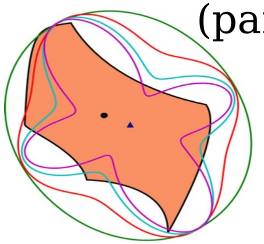

$[\boldsymbol{\Gamma}]_{ij} \propto$ components of weighted integrals of $\hat{\boldsymbol{\Gamma}}(\underline{\omega})$ evaluated at $2M$ wave numbers

So that the same $[\boldsymbol{\Gamma}]$ can be used for several realizations of $\Delta\mathbb{L}(\underline{x})$.

<u>1D validation:</u>

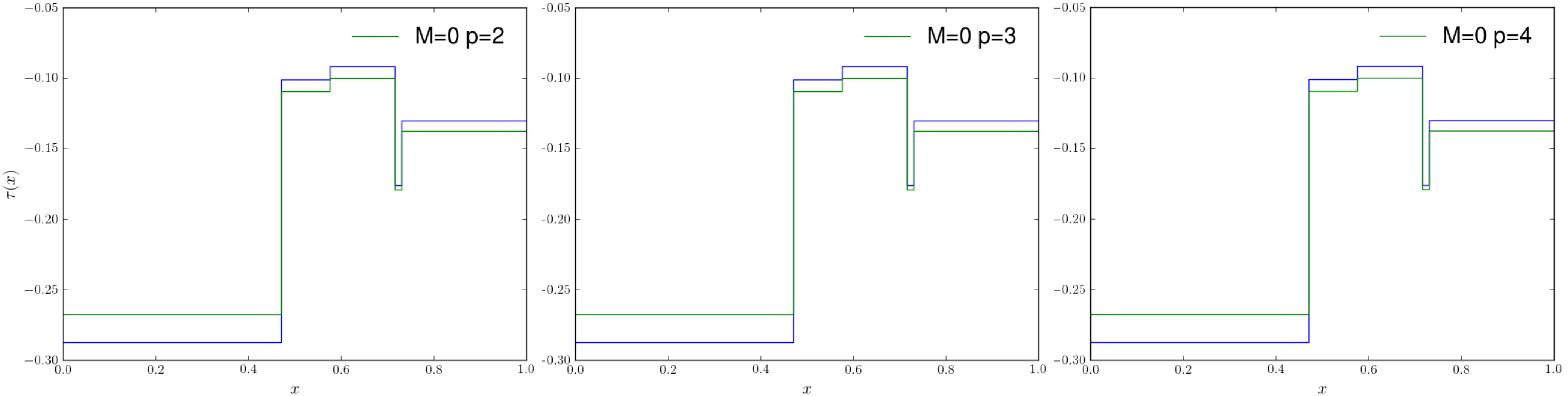

References

- **Brisard, S.** (2011). Analyse morphologique et homogénéisation numérique: application a la pâte de ciment. PhD thesis, *Université Paris-Est*.
- **Brisard, S., Dormieux, L., and Sab, K.** (2014). A variational form of the equivalent inclusion method for numerical homogenization. *International Journal of Solids and Structures, 51(3):716 – 728.*
- **Hashin, Z. and Shtrikman, S.** (1962). On some variational principles in anisotropic and nonhomogeneous elasticity. *Journal of the Mechanics and Physics of Solids, 10(4):335–342.*
- **Kröner, E.** (1972). Statistical continuum mechanics. *Springer-Verlag, Wien*.
- **Ponte-Castaneda, P. and Willis, J.** (1995). The effect of spatial distribution on the effective behavior of composite materials and cracked media. *Journal of the Mechanics and Physics of Solids, 43(12):1919–1951.*
- **Schröder-Turk, G., Kapfer, S., Breidenbach, B., Beisbart, C., and Mecke, K.** (2010). Tensorial Minkowski functionals and anisotropy measures for planar patterns. *Journal of Microscopy, 238(1):57–74.*
- **Teferra, K. and Graham-Brady, L.** (2015). Tessellation growth models for polycrystalline microstructures. *Computational Materials Science, 102:57–67.*
- **Vannucci, P.** (2016). Another View on Planar Anisotropy: The Polar Formalism, *pages 489–524. Springer International Publishing, Cham.*
- **Willis, J.** (1977). Bounds and self-consistent estimates for the overall properties of anisotropic composites. *Journal of the Mechanics and Physics of Solids, 25(3):185–202.*

Extra-slide #1 – Viscoplastic polycrystal model

- Constitutive model: $\dot{\boldsymbol{\sigma}}(t) = \mathbb{L} : [\dot{\boldsymbol{\varepsilon}}(t) - \dot{\boldsymbol{\varepsilon}}^p(t)]$

$$\dot{\boldsymbol{\varepsilon}}^p = \sum_{\alpha=1}^{2} \dot{\gamma}^{(\alpha)} \boldsymbol{\mu}^{(\alpha)} \qquad \boldsymbol{\mu}^{(\alpha)} = \underline{m}_\alpha \overset{s}{\otimes} \underline{n}_\alpha \qquad ,$$

$$\dot{\gamma}^{(\alpha)} = \dot{\gamma}_0^{(\alpha)} \left(\frac{|\boldsymbol{\sigma} : \boldsymbol{\mu}^{(\alpha)}|}{\tau^\alpha} \right)^{\frac{1}{m}} \mathrm{sgn}(\boldsymbol{\sigma} : \boldsymbol{\mu}^{(\alpha)}) \quad \dot{\tau}^\alpha = h \sum_{\beta=1}^{2} |\dot{\gamma}^{(\alpha)}|$$

- Material properties: 2D isotropic stiffness;
- Sources of randomness:
  - Grain morphology, lattice misorientation
- Quantity of interest: $p = \sum_{\alpha=1}^{2} \int_0^t |\dot{\gamma}^{(\alpha)}| \mathrm{d}\tau$

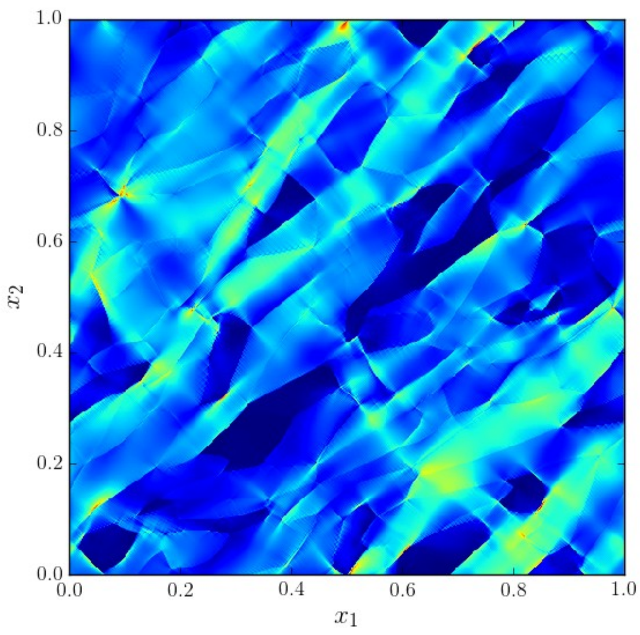

Extra-Slide #2 – Transform the problem

Solving for parameterizations of common curves $\mathcal{I}_{\alpha\gamma}$ is difficult. To circumvent this difficulty, we introduce a diffeomorphic transformation.

Let every point of a growing ellipse be given by a time-dependent mapping from a unit circle:

$$\varphi_\alpha : S^1 \times (0, \Delta) \to S_\alpha \subset \mathbb{R}^2$$
$$: (\underline{x}, t) \mapsto \underline{x}_\alpha + t\mathbf{Z}_\alpha^{-1/2} \cdot \underline{x}$$

We let the common curves be

$$\mathcal{I}_{\alpha\beta} = \{\underline{y} \in S_\alpha \cap S_\gamma \mid f_\gamma^\alpha(\underline{y}) = 0\}$$

with $f_\gamma^\alpha(\underline{y}) = \tau \circ \varphi_\alpha^{-1}(\underline{y}) - \tau \circ \varphi_\gamma^{-1}(\underline{y})$.

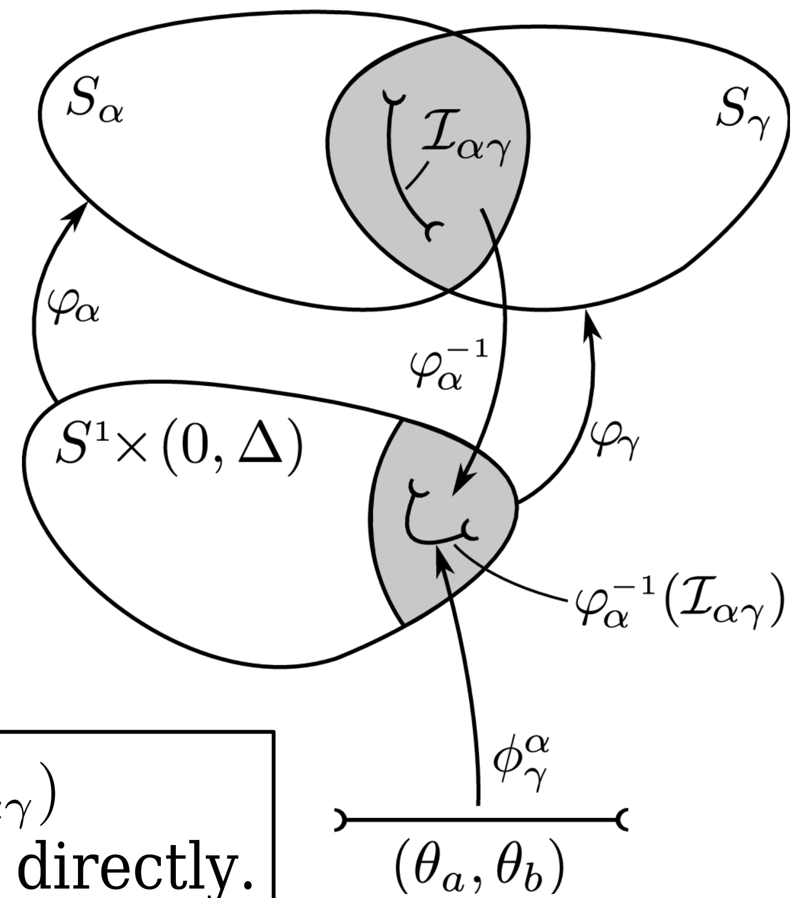

Finding parameterizations ϕ_γ^α of $\varphi_\alpha^{-1}(\mathcal{I}_{\alpha\gamma})$ is much easier than parameterizing $\mathcal{I}_{\alpha\gamma}$ directly.